at critical point $\partial^3 F(\phi_A)/\partial\phi_A{}^3 = 0$ or $\partial\chi_s(\phi_A)/\partial\phi_A = 0$.

$$\frac{\partial\chi_s(\phi_A)}{\partial\phi_A} = 0 = \frac{v_0}{2}\left(\frac{-1}{v_A\langle Z_A\rangle_w\phi_A{}^2} + \frac{1}{v_B\langle Z_B\rangle_w(1-\phi_A)^2}\right)$$

and

$$\phi_{A,critical} = \frac{(v_B\langle Z_B\rangle_w)^{1/2}}{(v_A\langle Z_A\rangle_w)^{1/2} + (v_B\langle Z_B\rangle_w)^{1/2}} \quad \text{(B2)}$$

This is eq 5 in the text.

References and Notes

(1) *Handbook of Elastomers*; Bhowmick, A. K., Stephens, H. L., Eds.; Marcel Dekker: New York, 1988.
(2) For example: Shibayama, M.; Yang, H.; Stein, R. S.; Han, C. C. *Macromolecules* **1985**, *18*, 2179.
(3) Bates, F. S.; Dierker, S. B.; Wignall, G. D. *Macromolecules* **1986**, *19*, 1938.
(4) ten Brinke, G.; Karasz, F. E.; MacKnight, W. J. *Macromolecules* **1983**, *16*, 1827.
(5) Kambour, R. P.; Bendler, J. T.; Bopp, R. C. *Macromolecules* **1983**, *16*, 753.
(6) Paul, D. R.; Barlow, J. W. *Polymer* **1984**, *25*, 487.
(7) Glinka, C. J.; Rowe, J. M.; LaRock, J. G. *J. Appl. Crystallogr.* **1986**, *19*, 427.
(8) Glinka, C. J., private communication.
(9) de Gennes, P.-G. *Scaling Concepts in Polymer Physics*; Cornell University Press: New York, 1979.
(10) Peebles, L. H., Jr. *Molecular Weight Distributions in Polymers*; Interscience: New York, 1970.
(11) Korstorz, G.; Lovesey, G. *Treatise on Materials Science and Technology*; Neutron *Scattering*; Academic Press: New York, 1979; Vol. 15, pp 5–8.
(12) Hong, K. M.; Noolandi, J. *Polym. Commun.* **1984**, *25*, 265.
(13) Rameau, A.; Gallot, Y.; Marie, P.; Farnoux, B. *Polymer* **1989**, *30*, 386.
(14) Ionescu, L.; Picot, C.; Duval, M.; Puplessix, R.; Benoit, H.; Cotton, J. P. *J. Polym. Sci., Poly. Phys. Ed.* **1981**, *19*, 1019.
(15) Mori, K.; Tanaka, H.; Hasegawa, H.; Hashimoto, T. *Polymer*, in press.
(16) Joanny, J. F. *C. R. Hebd. Seances Acad. Sci.* **1978**, *286B*, 89.
(17) Han, C. C.; Bauer, B. J.; Clark, J. C.; Muroga, Y.; Matsushita, M.; Okada, M.; Tran-Cong, Q.; Chang, T.; Sanchez, I. C. *Polymer* **1988**, *29*, 2002.
(18) Mays, J.; Hadjichristidis, N.; Fetters, L. J. *Macromolecules* **1984**, *17*, 2723.
(19) Sakurai, S.; Hasegawa, H.; Hashimoto, T.; Han, C. C., paper in preparation.
(20) Hayashi, H.; Flory, P. J.; Wignall, G. D. *Macromolecules* **1983**, *16*, 1328.
(21) Joanny, J. F. *J. Phys. A* **1978**, *11*, L117.
(22) de Gennes, P.-G. *J. Phys. Lett.* **1977**, *38*, L441.
(23) Binder, K. *J. Chem. Phys.* **1983**, *79*, 6387.
(24) Han, C. C. *Molecular Conformation and Dynamics of Macromolecules in Condensed Systems*; Nagasawa, M., Ed.; Elsevier: New York, 1988.
(25) Fetters, L. J., private communication.
(26) Balazs, A. C.; Sanchez, I. C.; Epstein, I. R.; Karasz, F. E.; MacKnight, W. J. *Macromolecules* **1985**, *18*, 2188.
(27) Balazs, A. C.; Karasz, F. E.; MacKnight, W. J.; Ueda, H.; Sanchez, I. C. *Macromolecules* **1985**, *18*, 2784.

Registry No. PBD, 9003-17-2; neutron, 12586-31-1.

Phase Separation Dynamics of Rubber/Epoxy Mixtures

Hak-soo Lee and Thein Kyu*

Center for Polymer Engineering, University of Akron, Akron, Ohio 44325.

Received March 20, 1989; Revised Manuscript Received June 16, 1989

ABSTRACT: Time-resolved light scattering has been employed to investigate the kinetics of phase separation in mixtures of carboxyl-terminated butadiene–acrylonitrile copolymer (CTBN) and diglycidyl ether bisphenol A (DGEBA) epoxy oligomers. The CTBN/DGEBA mixture reveals an upper critical solution temperature (UCST); i.e., the mixture phase separates upon cooling but reverts to a single phase upon heating. Several temperature- (T-) quench experiments with various quenched depths were undertaken on a 20 wt % CTBN mixture. The time evolution of scattering halo was subsequently followed as a function of quenched depth. At deep quenches, the phase separation process has been dominated by spinodal decomposition (SD). The general trend of SD is nonlinear in character. The evolution of the maximum wavenumber (q_m) and the corresponding maximum intensity (I_m) obey the power law ($q_m \sim t^{-\varphi}$ and $I_m \sim t^{\psi}$). The exponent φ exhibits quench depth dependence with the value varying from 1/6 to 1/3. The results were further tested with the dynamic scaling laws.

Introduction

Rubber-modified plastics have been the subject of continued interest in the field of polymer alloys. Thermoset epoxy resins are generally known to be brittle. Hence, the utilization of epoxy as a neat resin is not practical in many industrial applications. However, a slight addition of rubbery components into epoxy resins has been shown to improve mechanical properties of the materials, particularly toughness.[1] Since then, there have been numerous studies in the literature on the rubber-modified epoxies.[2–8]

It has been realized that the extent of improvement critically depends upon the size of rubbery particles, their dispersion, and interfacial adhesion between the dispersed rubbery phase and the matrix. The final morphology of the cured system depends on the competition between the cross-linking reaction and phase decomposition during curing. The understanding of reaction kinetics and phase separation dynamics is of crucial importance in order to achieve an optimum phase structure. In this study, the kinetic behavior of CTBN/DGEBA oligomer mixtures has been explored exclusively without adding any cross-linking agents.

Experimental Section

The epoxy resin used in this study was a diglycidyl ether Bisphenol A (DGEBA) supplied by the Shell Co. (Epon 828, $M_n \cong 380$). The elastomeric modifier, provided by the B.F. Goo-

* To whom correspondence should be addressed.

0024-9297/90/2223-0459$02.50/0

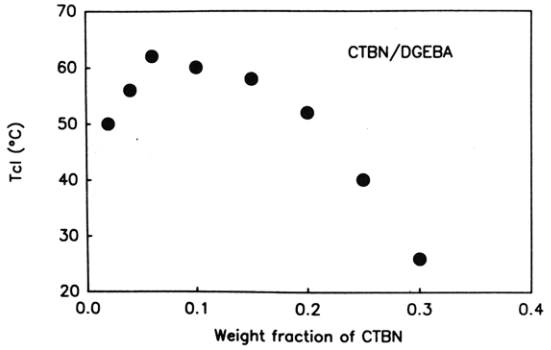

Figure 1. Equilibrium phase diagram for CTBN/DEGBA mixtures.

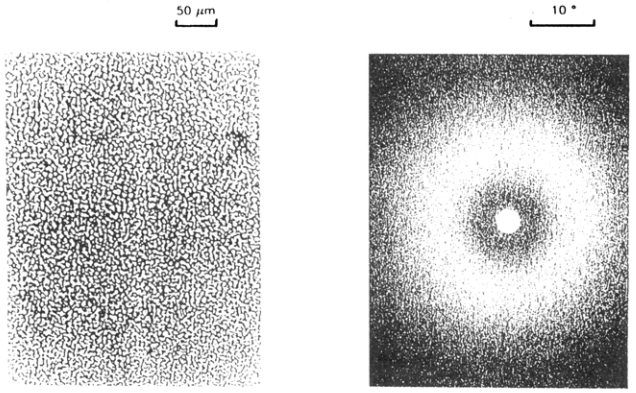

Figure 2. An optical micrograph of 20 wt % CTBN mixture revealing interconnected domains and the corresponding scattering halo during spinodal decomposition.

drich Co., was a carboxyl-terminated butadiene–acrylonitrile copolymer (CTBN) containing 17 wt % acrylonitrile with a molecular weight of $M_n \cong 3{,}500$. The mixtures were prepared by stirring at about 80 °C for 10 min and then transferred to oval type glass slides. Bubbles were then removed in a vacuum oven at about 80 °C until the specimen was, at least, visually bubble-free. A glass cover was placed on the liquid mixture and cooled down to ambient temperature.

The cloud point phase diagram was established by using a light scattering setup described elsewhere.[9] This setup consists of a He–Ne laser light source with a wavelength of 632.8 nm. The scattered intensity was monitored by a two-dimensional Vidicon detector interlinked with an Optical Multichannel Analyzer (OMA III, Model 1460, EG & G Princeton Applied Research Co.). A couple of heating cells were used for time evolution scattering studies: one was controlled at the experimental temperature while the other was used for preheating. Several temperature quench experiments were undertaken from a single-phase (57 °C) to a two-phase region (34–48 °C). A number of reverse temperature jumps were also carried out from 40 °C to a single-phase region 53–59 °C).

Results and Discussion

Phase Equilibria. Cloud point measurements of CTBN/DGEBA oligomer mixtures were conducted at various heating rates of 1, 0.5, 0.1, and 0.05 °C/min. The data were extrapolated to the zero heating rate to establish the cloud point temperature versus composition phase diagram. As can be seen in Figure 1, the phase diagram is an upper critical solution temperature (UCST) in character with a maximum at 6 wt % of CTBN and at 60 °C. The phase separation process is reversible as is typical for low molecular weight oligomer mixtures.[10,11]

When the liquid mixture of 20/80 CTBN/DGEBA was suddenly brought from a single phase (53 °C) to an unstable two-phase region (23 °C), a highly interconnected structure appears under optical microscope. The domain size

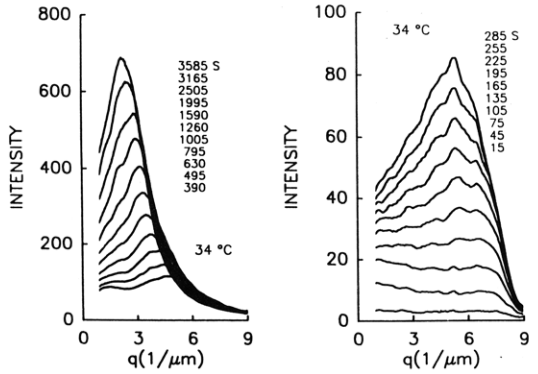

Figure 3. Time evolution of scattering peaks following a temperature quench from 57 to 34 °C.

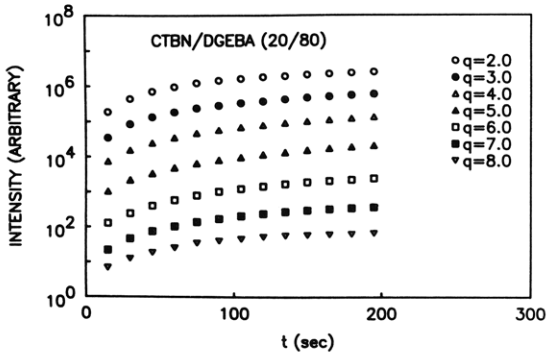

Figure 4. Logarithmic intensity versus time plots for 20 wt % CTBN mixtures at various scattering wavenumbers.

gets larger with elasped time. In light scattering studies, a scattering halo corresponding to the average periodic distance of phase-separated domains develops and then collapses to a smaller diameter. Figure 2 exhibits such an optical micrograph and a scattering halo of the 20 wt % CTBN mixture. These are the familiar characteristics of phase separation by spinodal decomposition (SD).[12]

Early Stage of SD. Several T-quench experiments were undertaken to elucidate the dynamics of phase separation in the 20/80 CTBN/DGEBA mixture. Figure 3 shows time evolution of a scattering peak following a T quench from 57 to 34 °C. The scattering maximum first appears at a large wavenumber ($q \sim 6.5\ \mu m^{-1}$), and the peak position remains virtually invariant for a short period; i.e. it shows little or no movement. At a later time, the peak shifts to lower wavenumbers due to the phase growth. The peak movement at the early stage of SD is so small so much so that it may be worthy of testing with the linearized theory of Cahn–Hilliard,[13,14] which predicts an exponential growth of a scattering function, i.e.

$$I(q,t) = I(q,t=0)\exp\{2R(q)t\} \quad (1)$$

where t is the phase separation time and q the scattering wavenumber defined as $q = (4\pi/\lambda)\sin(\theta/2)$. λ and θ are the wavelength of light and the scattering angle measured in the medium, respectively. The amplification factor $R(q)$ that represents the growth of composition fluctuations of the mixture is further related by

$$R(q) = -Mq^2\{\partial^2 f/\partial c^2 + 2\kappa q^2\} \quad (2)$$

where f is the local free energy density, c the concentration, κ the coefficient of composition gradient, and M the mobility. The inadequacy of eq 1 was pointed out by Cook,[15] who modified the linear theory by incorporating thermal fluctuations of the stable single phase. The mod-

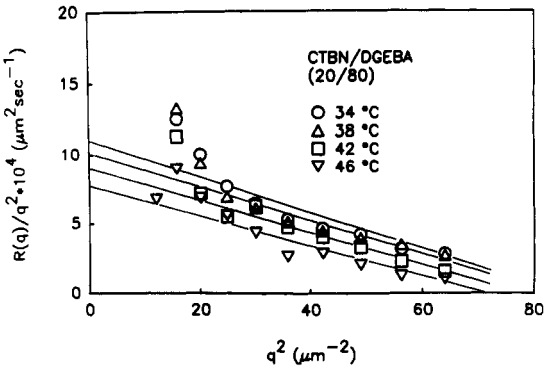

Figure 5. Cahn's plots of $R(q)/q^2$ versus q^2 for various temperature quenches.

ified equation is expressed as

$$I(q,t) = I_s(q) + [I(q,t=0) - I_s(q)] \exp\{2R(q)t\} \quad (3)$$

where

$$I_s(q) \sim S_s(q) \quad (4)$$

is a virtual structure function of the stable system. The plot of logarithmic scattered intensity against time exhibits an exponential increase for a limited period and then departs from the linear slope (Figure 4). The values of $R(q)$ were determined from the slopes and replotted in Figure 5 in accordance with eq 2, i.e., $R(q)/q^2$ versus q^2. The data can be approximated fairly well by linear slopes, except for a few points at low q. It should be pointed out that these data at low q are somewhat affected by the parasitic scattering arising from the beam stop. In our opinion, the validity of the linear theory should be further checked by the following equation

$$q_m^2 = (1/2)q_c^2 \quad (5)$$

where q_c is a crossover wavenumber and q_m is the maximum wavenumber. As can be seen in Figure 5, eq 5 appears to be valid, suggesting that the modified linearized theory may be valid for the early stage of SD. The validity of the linearized theory for the early stage of SD has been challenged by many investigators. Hashimoto and co-workers[16,17] were the first to show experimentally that there is an appreciable period where the scattering peak is invariant and $R(q)/q^2$ versus q^2 plots give linear slopes. Han et al.[18] also found the linear regime in the early stage of SD for polystyrene (PS)/poly(vinyl methyl ether) (PVME) blends. Recently, we also obtained a similar result for polycarbonate (PC)/poly(methyl methacrylate) (PMMA) mixtures.[19] Very recently, Bates[20] showed that the linearized theory is still applicable even if the time evolution of the structure function is weakly nonlinear; i.e., the scattering peak shows a very small movement. On the basis of cell dynamics, Oono and Puri[21] predicted the existence of a linear region in binary mixtures.

Phase Dissolution. The reversed experiments of temperature jumps from 40 to 53–57 °C were also undertaken. Figure 6 exhibits the decay of scattering curves, showing a slight movement of the peak to a lower scattering angle. The time required for the specimen to equilibrate at the experimental temperatures is approximately 5 s and is subtracted from the total phase dissolution time. A similar observation was made by Osamura et al.,[22] who reported the increase of periodic particle distance during reversion in Al–Zn alloys; i.e., the scattering angle shows a movement to lower scattering angles. The authors demonstrated that the behavior of reversion depends on the temperatures of T jumps, i.e., above and below the zone solvus. In the former, the scattered

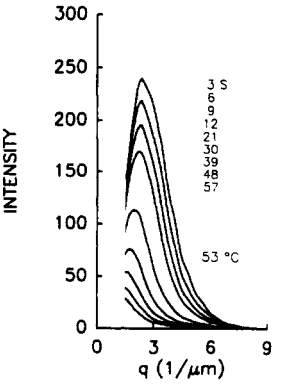

Figure 6. Time decay of scattering profiles of 20 wt % CTBN following a T jump from 40 to 53 °C.

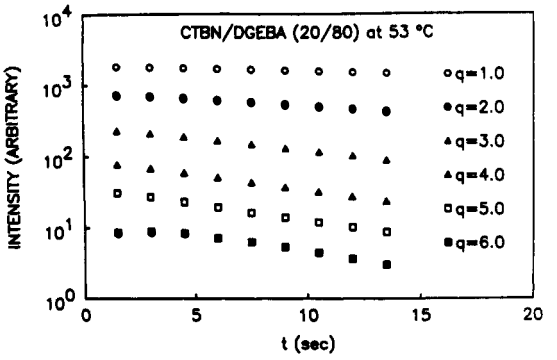

Figure 7. Logarithmic intensity versus time plots for 20 wt % CTBN during phase dissolution.

peak while moving to lower angles decreases rapidly and vanishes completely within 12 s, which is consistent with our observation. Below the zone solvus, the scattered intensity initially decreases, but after passing the minimum, it increases again. This implies that some components of the fluctuations that were growing during decomposition will begin to decay at the inversion temperature. Also, there will be an increase in the wavelength of the component receiving maximum amplification. Phase decomposition will continue although there may be an initial decrease in the degree of decomposition due to the decay of the short wavelength components. The authors concluded that it is due to the coarsening of the zones (domains) survived at the inversion temperature.

In the present case, since the peak movement is very small, it may be worthwhile to analyze in terms of the reverse linearized theory. The decay of scattered intensity was plotted as a function of phase dissolution time in semilogarithmic scale in Figure 7. The data are fairly linear for most wavenumbers, suggesting an exponential decay of scattered intensity. The decay rates, $R(q)$, were determined from the slopes and plotted against q^2 in Figure 8. The data can be fitted reasonably well with linear slopes from which the apparent diffusivities may be determined as demonstrated by Kumaki and Hashimoto[23] and Sato and Han[24] for PS/PVME blends. The latter authors[24] further pointed out that such q^2 dependence is only valid if the fluctuation size is sufficiently small. The temperature dependence of apparent diffusivities during dissolution was plotted in Figure 9 together with those of the decomposition. The solid line was drawn by using a non linear regression. The temperature at which the diffusivity becomes zero is regarded as spinodal temperature (T_S). The T_S is estimated to be 50 °C. Near the T_S, the diffusivity D_{app} may be scaled as

$$D_{app} = D_0\epsilon^{\nu} \quad (6)$$

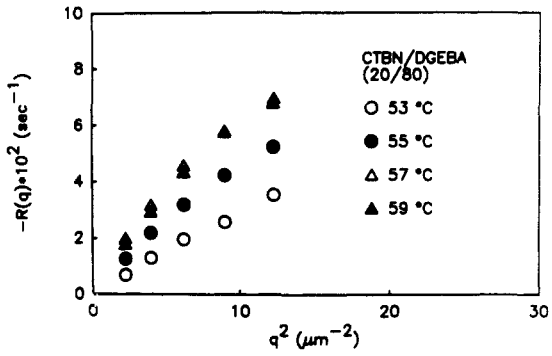

Figure 8. q^2 dependence of decay rate $R(q)$ of 20 wt % CTBN.

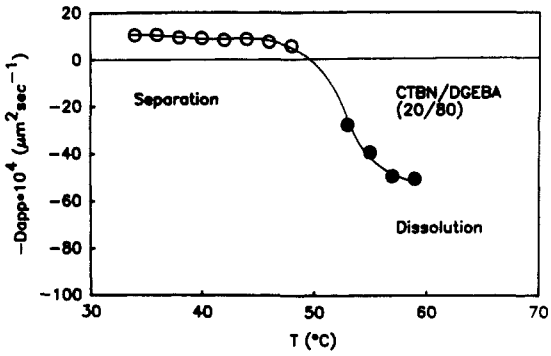

Figure 9. Temperature dependence of apparent diffusivities for various T quenches and T jumps for 20 wt % CTBN.

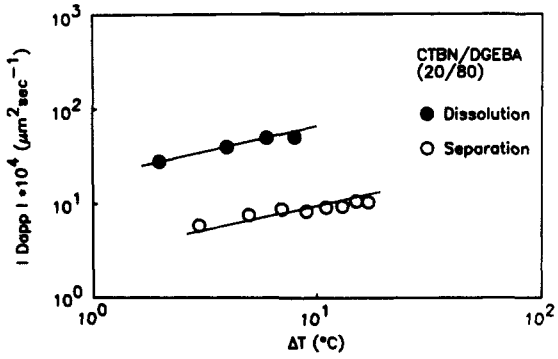

Figure 10. log–log plot of diffusivity as a function of ΔT (= $T - T_S$) for phase separation and dissolution for 20 wt % CTBN.

with

$$\epsilon = (T - T_S)/T_S \tag{7}$$

where D_0 is the self-diffusion coefficient and ν is the critical exponent which was measured for a number of low molecular weight solutions and was found to be 0.66.[25,26] Nojima et al.[27] obtained ν values around 0.75 for polystyrene (PS)/poly(methylphenylsiloxane) (PMPS) oligomer mixtures. In the present case, the value of ν is approximately 0.5 ± 0.1, thus close to the reported value for small molecular systems (Figure 10). Snyder et al.[12] and Hashimoto et al.[16] obtained $\nu = 1$ for the PS/PVME blends which is what is predicted by the linearized theory of Cahn–Hilliard. A similar exponent ($\nu = 1$) was also obtained by us for a hydroxylpropyl cellulose (HPC)/water system.[28]

Late Stages of SD. As pointed out previously, the late stage of SD in the CTBN/DGEBA mixture is nonlinear in character; thus it is reasonable to explain in terms of the power law relationships, namely

$$q_m(t) = t^{-\varphi} \tag{8}$$

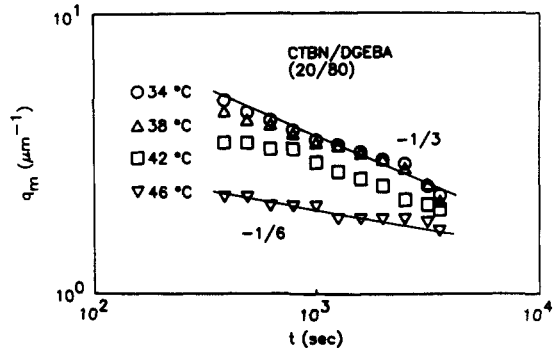

Figure 11. log–log plot of maximum wavenumber versus phase separation time.

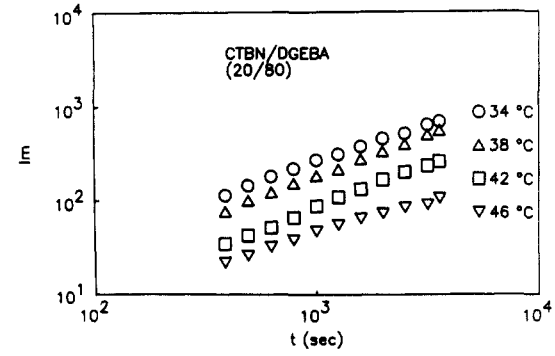

Figure 12. The corresponding plot of maximum intensity versus phase separation time.

$$I_m(t) = t^{\psi} \tag{9}$$

where the subscript m stands for the maximum values. The exponents φ and ψ are predicted by various authors.[29-34] Langer, Baron, and Miller (LBM),[29] based on the nonlinear statistical consideration, obtained the value of $\varphi = 0.21$. Binder and Stauffer,[30] who considered the coalescence of cluster domains, predicted a relationship $\psi = 3\varphi$ with the values of $\varphi = 1/3$ and $\psi = 1$. On the basis of the percolation approach by taking into consideration the diffusion and hydrodynamic flow, Siggia[31] obtained the same equation, but with $\varphi = 1/3$ for the early growth regime and $\varphi = 1$ for the intermediate stage (flow stage).

Figures 11 and 12 exhibit the log–log plots of the maximum wavenumber and the corresponding scattered intensity versus phase separation time, respectively. At shallow quenches, the q_m is initially constant for a certain period, representing the linear regime. Then, the value of φ varies from 1/6 to 1/4 depending on the quench depth, implying the change in the mechanism of phase decomposition. At deep quenches, the growth process proceeds faster with exponents of $\varphi = 1/3$ and $\psi = 1$, which is in good accord with the prediction of cluster dynamics.[14] The crossover of 1/6 to 1/3 at a given temperature has also been observed by Katano and Iizumi for Fe–Cr alloys.[36] According to Binder,[30] the exponent φ varies with $1/(d + 3)$ for the surface mobility and $1/(d + 2)$ for the bulk mobility. Furukawa[32] generalized the kinetic exponents to vary as $1/(d + 2 + \zeta - h)$ in order to explain various crossover processes. The two new parameters ζ and h may assume different values depending on the growth mechanism that is dominant. Our experiment is not long enough to observe the very late stage of SD where φ varies with a value of 1 (i.e. percolation regime)[31] and then slows down to 1/6 due to the pinning effect. We felt that the scaling law may not be opera-

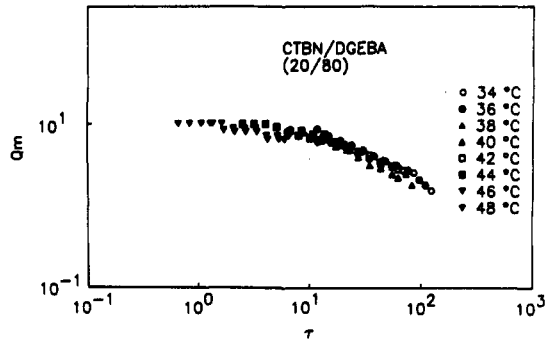

Figure 13. A universal master curve with dimensionless variables Q_m vs τ.

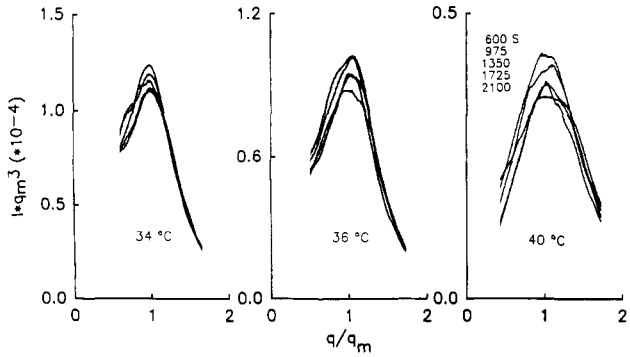

Figure 14. A plot of $I(q)q_m^3$ versus q/q_m for self-similarity test.

tive over the whole phase separation process as pointed out by Kawasaki and Ohta.[33]

Since there is an appreciable period at which the scattering wavenumber q_m appears constant, the correlation length (ξ) in the single phase may be approximated as the initial fluctuation size of SD at $t = 0$

$$\xi = 1/q_m(t = 0) \tag{10}$$

The universal curve may then be established with dimensionless variables Q_m and τ, which may be scaled as

$$Q_m = q\xi \tag{11}$$

$$\tau = D\xi^{-2}t \tag{12}$$

where D and ξ were already known experimentally from Figures 4 and 5. As can be seen in Figure 13, the superposition of universal curve appears reasonable. The time scale is rather short, but the trend is similar to those of metal alloys, solution mixtures, polymer blends, among others.[35]

Scaling of Self-Similarity. Next, we shall examine the time evolution of scattering function for self-similarity.[37] Since the scaled structure function $\tilde{s}(z)$ is a Fourier transform of the space correlation function of the composition, it is related to the scattered intensity $I(q,t)$ at a given time t

$$I(q,t) \sim V\langle\eta^2\rangle\xi(t)^3\tilde{s}(z) \tag{13}$$

with

$$z = q\xi(t) \tag{14}$$

where V is the irradiated volume and $\langle\eta^2\rangle$ the mean-square fluctuations of refractive indices. Here, $\xi(t)$ in turn relates to the wavelength of periodic structure $\Lambda(t)$ by the following equation

$$\xi(t) = \Lambda(t)/2\pi = 1/q_m(t) \tag{15}$$

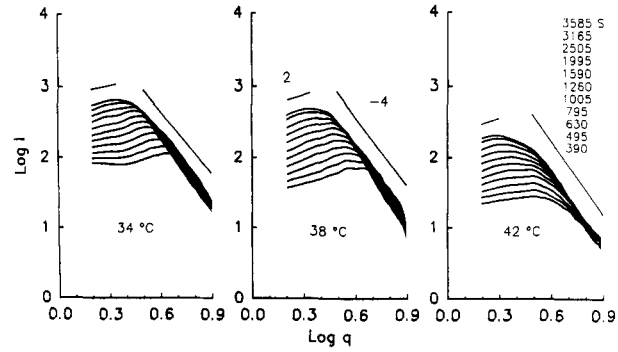

Figure 15. log–log plot of scattering function versus scattering wavenumber for various time scale.

From eq 13 to eq 15, the structure function $\tilde{s}(z)$ can be described as

$$\tilde{s}(z) \sim I(q,t)q_m^3(t) \tag{16}$$

In the early stage of SD, $\langle\eta^2(t)\rangle$ is not necessarily constant; therefore it cannot be scaled by a single length parameter $\xi(t)$. We therefore employed the data at late stages of SD in this scaling test. As shown in Figure 14, the plot of $\tilde{s}(z)$ versus z gives a good superimposed master curve for different phase separation times, suggesting that self-similarity is attained when the structure function exhibits temporal universality.

Scaled Structure Functions. Next, the shape of the scattering function has been analyzed in accordance with the recent scaling theory of Furukawa,[38] i.e.

$$S(x) = \frac{(1 + \gamma/2)x^2}{\gamma/2 + x^{2+\gamma}} \tag{17}$$

where $x = qr$. For the critical composition, $\gamma = 2d$ and at off-critical composition $\gamma = d + 1$ with d being the dimensionality of growth. The shape of the scattered intensity is predicted as $I \sim q^2$ at $q < q_m$ and $I \sim q^{-\gamma}$ at $q > q_m$. For three-dimensional growth, γ is equal to 6 for the critical composition and 4 for off-critical mixtures. Figure 15 shows the log–log plots of intensity versus wavenumber for the 20 wt % CTBN mixture. The value of γ is approximately 4, suggesting that the SD process of the 20 wt % CTBN is reminiscent of the behavior of off-critical mixtures. The slopes of 2 and −4 have been reported for metal alloys,[39] oligomer mixtures,[40] and polymer solutions.[27] In the case of critical mixture of polystyrene and poly(vinyl methyl ether), Hashimoto et al.[41] obtained the values of 2 and −6. Very recently, we also observed the slopes of 2 and −6 for the critical mixture of PC/PMMA.[42] Furukawa[32] postulated that $\gamma = 6$ may be valid only for intermediate wavenumbers; at larger q the exponent recovers the Porod value of 4. The recovery of q^{-4} dependence was already confirmed experimentally in metal alloys[43] and in polymer blends.[44] Very recently, Oono and Puri[21] showed in their simulation based on a nondifferential kinetic equation that the slope could be much steeper than q^{-4} at intermediate wavenumbers of the percolated regime.

Conclusions

Phase separation occurs by spinodal decomposition in the mixtures of rubber and epoxy. The linearized Cahn–Hilliard theory appears to be operative for the early stage of SD. The kinetic exponent shows a temperature (ΔT) dependence with the values changing from −1/6 to −1/3. The universal curve of the present CTBN/DGEBA appears similar to those for solution mixtures, oligomer,

and some polymer blends. Self-similarity is attained in the regime where the structure function shows universality with time. The phase separation dynamics of the 20 wt % CTBN is reminiscent of the behavior of off-critical mixtures.

Registry No. Epon 828, 25068-38-6.

References and Notes

(1) McGarry, F. J.; Willner, A. M. *Org. Coat. Plast. Chem.* **1968**, *28*, 512.
(2) Visconti, S.; Marchessault, R. H. *Macromolecules* **1974**, *7*, 913.
(3) Boisserie, C.; Marchessault, R. H. *J. Polym. Sci., Polym. Phys. Ed.* **1977**, *15*, 1211.
(4) Gillham, J. K. *Polym. Eng. Sci.* **1979**, *19*, 676.
(5) Wang, T. T.; Zupko, H. M. *J. Appl. Polym. Sci.* **1981**, *26*, 2391.
(6) LeMay, J. D.; Kelley, F. N. *Adv. Polym. Sci.* **1986**, *78*, 115.
(7) Chan, L. C.; Gillham, J. K.; Kinloch, A. J.; Shaw, S. J. *Adv. Chem. Ser.* **1984**, *No. 208*, 235, 261.
(8) Yee, A. F.; Pearson, R. A. *J. Mater. Sci.* **1986**, *21*, 2462, 2475.
(9) Kyu, T.; Saldanha, J. M. *J. Polym. Sci., Polym. Lett. Ed.* **1988**, *26*, 33.
(10) Nojima, S.; Nose, T. *Polym. J.* **1982**, *14*, 269.
(11) Russel, T. P.; Hadziioannou, G.; Warburton, W. K. *Macromolecules* **1985**, *18*, 78.
(12) Snyder, H. L.; Meakin, P.; Reich, S. *Macromolecules* **1983**, *16*, 757.
(13) Cahn, J. W. *J. Chem. Phys.* **1965**, *42*, 93; *Trans Metall. Soc. AIME* **1968**, *242*, 1649.
(14) Hilliard, J. E. In *Phase Transformations* ASME, Oct 1968, p 497.
(15) Cook, H. E. *Acta Metall.* **1970**, *18*, 297.
(16) Hashimoto, T.; Kumaki, J.; Kawai, H. *Macromolecules* **1983**, *16*, 641.
(17) Takenaka, M.; Izumitani, T.; Hasimoto, T. *Macromolecules* **1987**, *20*, 2257.
(18) Okada, M.; Han, C. C. *J. Chem. Phys.* **1985**, *85*, 5317.
(19) Kyu, T.; Saldahna, J. M. *Macromolecules* **1988**, *21*, 1021.
(20) Bates, F. S. *Bull. Am. Phys. Soc.* **1989**, *34*, 653.
(21) Oono, Y.; Puri, S. *Phys. Rev. Lett.* **1987**, *58*, 836.
(22) Osamura, K.; Okuda, H.; Amemiya, Y.; Hashizume, H. In *Dynamics of Ordering Processes in Condensed Matter*; Komura, S., Furukawa, H. Ed.; Plenum: New York, 1989, p 273.
(23) Kumaki, J.; Hashimoto, T. *Macromolecules* **1986**, *19*, 763.
(24) Sato, T.; Han, C. C. *J. Chem. Phys.* **1988**, *88*, 2057.
(25) Kuwahara, N.; Fenly, D. V.; Tamsky, M.; Chu, B. *J. Chem. Phys.* **1970**, *55*, 1140.
(26) Chou, Y. C.; Goldburg, C. M. *Phys. Rev. A* **1981**, *24*, 3205.
(27) Nojima, S.; Ohyama, Y.; Yamaguchi, M.; Nose, T. *Polym. J.* **1982**, *14*, 907.
(28) Kyu, T.; Zhuang, P.; Mukherjee, P. *ACS Symp. Ser.* **1989**, *No. 384*, 266.
(29) Langer, J. S.; Baron, M.; Miller, H. S. *Phys. Rev. A* **1975**, *11*, 1417.
(30) Binder, K.; Stauffer, D. *Phys. Rev. Lett.* **1973**, *33*, 1006.
(31) Siggia, E. D. *Phys. Rev. A* **1979**, *20*, 595.
(32) Furukawa, H. *J. Appl. Crystallogr.* **1988**, *21*, 805.
(33) Kawasaki, K.; Ohta, T. *Prog. Theor. Phys.* **1978**, *59*, 1116.
(34) Binder, K. *Phys. Rev. B* **1977**, *15*, 4425.
(35) Snyder, H.; Meakin, P. *J. Chem. Phys.* **1986**, *85*, 6118.
(36) Katano, S.; Iizumi, M. in ref 22, p 321.
(37) Furukawa, H. *Phys. Rev. Lett.* **1979**, *43*, 136.
(38) Furukawa, H. *Physica A (Amsterdam* **1984**, *123*, 497.
(39) Komura, S.; Osamura, K.; Fujii, H.; Takeda, T. *Phys. Rev. B* **1984**, *30*, 2944; **1985**, *31*, 1278.
(40) Takahashi, M.; Horiuchi, H.; kinoshita, S.; Ohyama, Y.; Nose, T. *J. Phys. Soc. Jpn.* **1988**, *55*, 2689.
(41) Hashimoto, T.; Itakura, M.; Hasegawa, H. *J. Chem. Phys.* **1986**, *85*, 6118.
(42) Lim, D. S.; Kyu, T. *Polym. Prepr. (Am. Chem. Soc., Div. Polym. Soc.)* **1988**, *29*, 354.
(43) Furusaka, M.; Fujikawa, S.; Sakaguchi, M.; Hirano, K. in ref 22, p 281.
(44) Hashimoto, T.; Takenaka, M.; Izumitani, T. *Polym. Commun.* **1989**, *30*, 45.

Orientational Order in Aramid Solutions Determined by Diamagnetic Susceptibility and Birefringence Measurements

Stephen J. Picken

AKZO Research Laboratories Arnhem, Corporate Research, Physical Chemistry Department, P.O. Box 9300, 6800 SB Arnhem, The Netherlands. *Received March 8, 1989; Revised Manuscript Received May 18, 1989*

ABSTRACT: Diamagnetic susceptibility and birefringence measurements on lyotropic solutions of poly(4,4′-benzanilidyleneterephthalamide) in concentrated sulfuric acid are presented. Three polymer samples, with different average molecular weight $\bar{M}_w$, were used. From these experiments the orientational order parameter $\langle P_2 \rangle$ is estimated. The experimental results are explained by a mean-field-type theory similar to the Maier–Saupe model for thermotropic liquid crystals. Molecular flexibility, concentration, and molecular weight are taken into account by using simple scaling factors.

I. Introduction

In this report some diamagnetic susceptibility and birefringence measurements are described on solutions of poly(4,4′-benzanilidyleneterephthalamide) (DABT, see Figure 1) in H_2SO_4. These measurements are used to estimate the orientational order parameter $\langle P_2 \rangle$. The $\langle P_2 \rangle$ order parameter is a measurement for the degree of molecular orientation.

In a previous publication[1] measurements of the nematic–isotropic transition temperature (clearing temperature) were reported as a function of polymer concentration and average molecular weight $\bar{M}_w$. In Figure 2 the experimental results for the clearing temperature of DABT solutions in H_2SO_4 are shown. The experiments were explained by a modified Maier–Saupe (mean-field) model, where the influence of molecular flexibility and polymer concentration was included using simple scaling factors in the strength of the potential. The model will be summarized in some detail.

The experiments described here can be explained by using the same model. The plan of this paper is as fol-

0024-9297/90/2223-0464$02.50/0